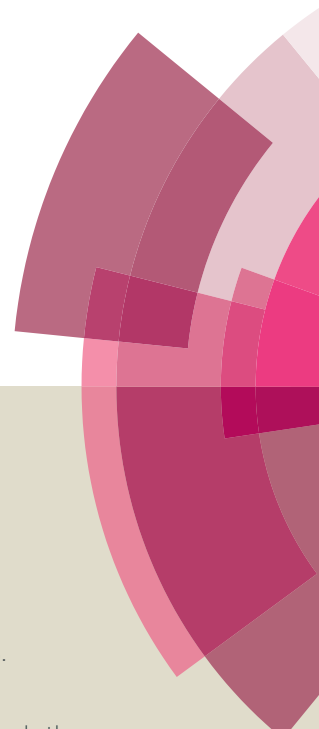


Catalysis Science & Technology

Accepted Manuscript



This article can be cited before page numbers have been issued, to do this please use: J. Comerford, S. Hart, M. North and A. C. Whitwood, *Catal. Sci. Technol.*, 2016, DOI: 10.1039/C6CY00134C.



This is an *Accepted Manuscript*, which has been through the Royal Society of Chemistry peer review process and has been accepted for publication.

Accepted Manuscripts are published online shortly after acceptance, before technical editing, formatting and proof reading. Using this free service, authors can make their results available to the community, in citable form, before we publish the edited article. We will replace this *Accepted Manuscript* with the edited and formatted *Advance Article* as soon as it is available.

You can find more information about *Accepted Manuscripts* in the [Information for Authors](#).

Please note that technical editing may introduce minor changes to the text and/or graphics, which may alter content. The journal's standard [Terms & Conditions](#) and the [Ethical guidelines](#) still apply. In no event shall the Royal Society of Chemistry be held responsible for any errors or omissions in this *Accepted Manuscript* or any consequences arising from the use of any information it contains.



Journal Name

ARTICLE

Homogeneous and silica-supported zinc complexes for the synthesis of propylene carbonate from propane-1,2-diol and carbon dioxide.

Received 00th January 20xx,
Accepted 00th January 20xx

DOI: 10.1039/x0xx00000x

www.rsc.org/

James W. Comerford, Sam J. Hart, Michael North* and Adrian C. Whitwood

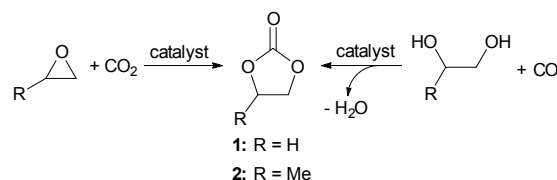
Three organozinc complexes have been synthesised and found to catalyse the carbonylation of propylene glycol with carbon dioxide to form propylene carbonate. A similar tethered organozinc complex was supported onto high loading aminopropyl functionalised hexagonal mesoporous silica and was also found to be catalytically active.

Introduction

Five-membered ring cyclic carbonates such as ethylene carbonate **1** and propylene carbonate **2** are of growing commercial importance due to their wide range of applications. These include: use as electrolytes for lithium ion batteries,¹ monomers for polymer synthesis,² intermediates in the production of dimethyl carbonate³ and anhydrous ethylene glycol,⁴ and green polar aprotic solvents with the potential to replace traditional solvents such as DMF, DMSO, NMP and acetonitrile.⁵

The commercially most important route for the synthesis of cyclic carbonates is the addition of carbon dioxide to epoxides (Scheme 1).⁶ Despite the 100% atom economy of this synthesis and the mild reaction conditions applicable to some of the more active aluminium catalysts,⁷ use of volatile epoxides as starting materials is problematic due to their toxicity and explosive potential. Consequently, the use of 1,2-diols as substrates for the synthesis of five-membered cyclic carbonates has been highlighted as a particularly attractive route with urea, alkyl carbonates and carbon dioxide being used as green carbonyl sources.⁸ Diols tend to have low toxicity and can often be sourced from renewable bio-derived resources, thus reducing environmental impact and moving away from dependence on oil based feedstocks. However, direct use of 1,2-diols and carbon dioxide to synthesise cyclic carbonates is thermodynamically unfavourable⁹ and requires high reaction temperatures, pressures and a water scavenger to shift the equilibrium towards formation of product.¹⁰ We recently reported that zinc triflate is a highly active catalyst for this reaction under relatively mild reaction conditions.¹¹ Although zinc triflate is significantly more active than other

homogeneous catalysts reported to date,¹² it lacked reusability which reduced its catalytic effectiveness.



Scheme 1: Routes to cyclic carbonates

Few heterogeneous catalysts have been developed for the carbonylation of diols with carbon dioxide, with two of the most active being reported by Tomishige; potassium iodide supported on zinc oxide and cerium oxide used with 2-cyanopyridine as co-catalyst/dehydrating agent.¹³ Despite some impressive conversions, the very specific particle sizes of the cerium oxide required for high activity and the mandatory use of 2-cyanopyridine makes the process expensive and difficult to implement on an industrial scale. As such, we report herein our investigation into the possibility of immobilising the previously reported zinc triflate catalyst by coordination with tethered bidentate ligands and our discovery of three homogeneous organozinc complexes with good catalytic activity. Many homogeneous zinc-ligand complexes of this type have been reported, often as initiators for the ring-opening polymerisation of lactides,^{14,15} but such complexes have not been reported as catalysts for the synthesis of cyclic carbonates.

Results and discussion

Building on our previous publication,¹¹ the initial focus was directed at assessing how co-ordination of zinc triflate to a variety of ligands would affect the catalytic activity of the complex. To investigate this, 5 mol% of ligand **3-14** (chart 1) was added to 5 mol% of zinc triflate and used for the synthesis of propylene carbonate from propylene glycol and carbon

Department of Chemistry, The University of York, Heslington, York, YO10 5DD (UK).
Fax: +44 1904-322-705; Tel: +44 1904-324-545; E-mail: michael.north@york.ac.uk.

Electronic Supplementary Information (ESI) available: Copies of NMR, mass and DRIFTS spectra, porosimetry data and X-ray data. See DOI: 10.1039/x0xx00000x

ARTICLE

Journal Name

dioxide, giving the results shown in Table 1. The relatively mild reaction conditions (135 °C, 40 bar CO₂ pressure) were developed during our previous study.

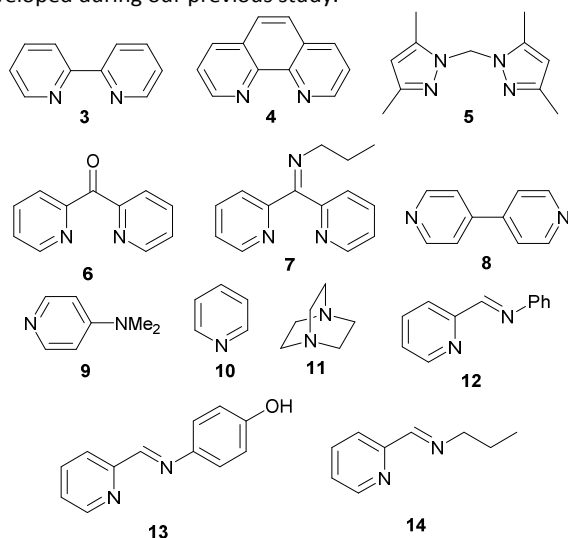


Chart 1: Structures of ligands 3-14

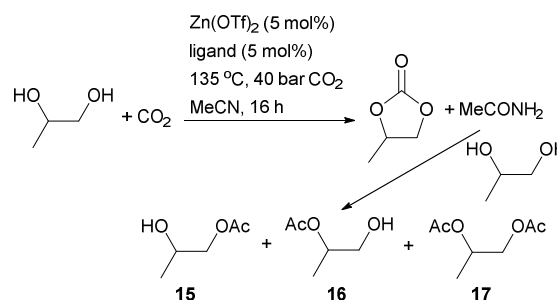
Table 1: Zinc complexes as homogeneous catalysts for propylene carbonate synthesis.

Entry	Zinc salt	Ligand ^a	2 (%)	By-products (%) ^b
1	-	-	0	0
2	Zn(OAc) ₂	-	12	10
3	Zn(OTf) ₂	-	42	40
4	Zn(OTf) ₂	3	30	29
5 ^c	Zn(OTf) ₂	3	32	30
6	Zn(OTf) ₂	4	32	30
7	Zn(OTf) ₂	5	39	40
8	Zn(OTf) ₂	6	0	0
9	Zn(OTf) ₂	7	30	28
10	Zn(OTf) ₂	8	27	26
11	Zn(OTf) ₂	9	26	26
12	Zn(OTf) ₂	10	26	25
13	Zn(OTf) ₂	11	30	28
14	Zn(OTf) ₂	12	31	29
15	Zn(OTf) ₂	13	0	0
16	Zn(OAc) ₂	13	0	0
17	Zn(OTf) ₂	14	31	30
18	Zn(OAc) ₂	14	3	1

a) Control reactions showed that ligands 3–14 themselves had no catalytic activity. b) Combined yield of mono- and di-esters of propylene glycol. c) 10 mol% of ligand **3** used.

Acetonitrile was found to be the most effective solvent and chemical water trap, though the initially formed acetamide by-product reacted with some of the diol starting material to give a mixture of mono and di-acetate by-products **15–17** (Scheme 2).

Entries 1-3 of Table 1 are control experiments showing that no reaction occurred in the absence of zinc salt and benchmarking the catalytic activity of zinc acetate and triflate in the absence of ligand. Additional control experiments were carried out using ligands **3–14** in the absence of any zinc salt,

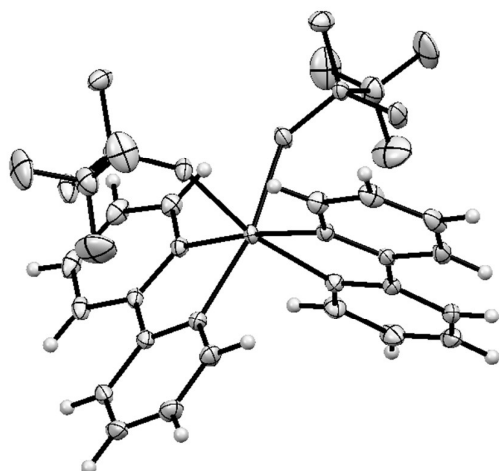
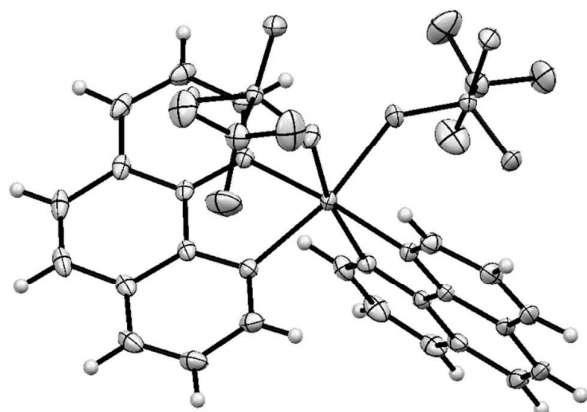
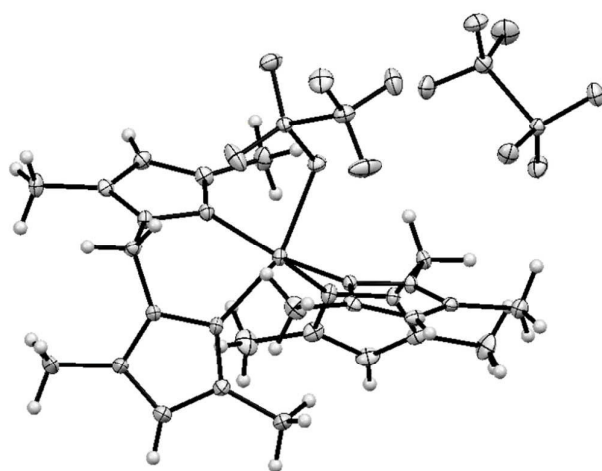


Scheme 2: Formation of acetate by-products

but in all these cases no propylene carbonate was formed. Entries 2 and 3 confirm the enhanced catalytic activity associated with zinc triflate compared to zinc acetate, an effect which is consistent with a need to maximise the Lewis acidity of the zinc ion. The use of ligands **3–14** with zinc triflate caused notable reductions in the conversion to propylene carbonate compared to the use of zinc triflate without ligand. This is also consistent with a reduction in Lewis acidity of the zinc ion due to the presence of an electron donating ligand, though steric effects may also have an influence.

The majority of the reactions catalysed by zinc triflate and a potentially bidentate ligand gave conversions of 30-32%, though the highest (39%) was achieved using methylenebis-3,5-dimethylpyrazole **5** (entry 7). Monodentate ligands gave lower conversions and no propylene carbonate formation was observed when using either 2,2'-dipyridyl ketone **6** (entry 8) or *p*-[(2-pyridylmethylene)amino]-phenol **13** (entries 15 and 16). The inhibition of catalytic activity seen when using oxygen containing ligands suggests the ketone/phenol competitively binds with the zinc, preventing its interaction with carbon dioxide and/or diol. Varying the zinc counter ion (acetate vs triflate) did not change the lack of conversion observed with ligand **13** (entries 15 and 16). However, removal of the oxygen containing groups from the ligands by substituting 2,2'-dipyridyl ketone **6** with 2,2'-dipyridyl-*N*-propyl imine **7** and substituting *p*-[(2-pyridylmethylene)amino]-phenol **13** with 2-(*N*-phenylformimidoyl)-pyridine **12** restored the catalytic activity of the zinc complexes, giving 30% and 31% conversion respectively, (entries 9 and 14). Increasing the ratio of 2,2'-bipyridine ligand **3** to zinc triflate from 1:1 to 2:1 had no significant effect on the conversion (entries 4 and 5) which is consistent with a 1:1 zinc-ligand species being the active catalyst. The importance of the zinc counter ion in the complexes is shown by entries 17 and 18 in which the triflate complex gave ten times high conversion than the acetate complex. This is consistent with the need to have a counterion which is a good leaving group to reduce competition for coordination zinc between the counterion and the propylene glycol.

Three of the systems which gave some of the highest conversions (entries 4, 6 and 7) were chosen for further study by preparing, isolating and characterising the complex prior to its use as a catalyst. Use of ligands **3** and **4** resulted in the formation of known¹⁵ octahedral complexes of formula [Zn(**3** or **4**)₂(CF₃SO₃)₂] which were characterised by X-ray

Figure 1: Ortep diagram of $[\text{Zn}(\mathbf{3})_2(\text{CF}_3\text{SO}_3)_2]$ Figure 2: Ortep diagram of $[\text{Zn}(\mathbf{4})_2(\text{CF}_3\text{SO}_3)_2]$ Figure 3: Ortep diagram of $[\text{Zn}(\mathbf{5})_2(\text{CF}_3\text{SO}_3)]^+ (\text{CF}_3\text{SO}_3)^-$

crystallography (Figures 1 and 2) with bond lengths and angles closely similar to those reported previously.[‡] In contrast, use of ligand **5** resulted in formation of a five-coordinate zinc species which was characterised by X-ray crystallography[‡] as

Table 2: Selected bond lengths and angles for the zinc complexes of ligands **3–5**.

Bond	Bond length (Å) or bond angle (°)		
	$[\text{Zn}(\mathbf{3})_2(\text{CF}_3\text{SO}_3)_2]$	$[\text{Zn}(\mathbf{4})_2(\text{CF}_3\text{SO}_3)_2]$	$[\text{Zn}(\mathbf{5})_2(\text{CF}_3\text{SO}_3)]^+ (\text{CF}_3\text{SO}_3)^-$
Zn1–O1	2.1823(9)	2.1875(9)	2.1671(18)
Zn1–N1	2.1048(11)	2.1239(11)	2.047(2)
Zn1–N2	2.0972(11)	2.1036(11)	-
Zn1–N4	-	-	2.075(2)
Zn1–N5	-	-	2.083(2)
Zn1–N8	-	-	2.080(2)
N1–Zn1–N2	78.13(4)	79.31(4)	-
N1–Zn1–N4	-	-	91.12(9)
N5–Zn1–N8	-	-	88.54(9)

$[\text{Zn}(\mathbf{5})_2(\text{CF}_3\text{SO}_3)]^+ (\text{CF}_3\text{SO}_3)^-$ (Figure 3). This complex could also be prepared from a 1:1 ratio of ligand **5** and zinc triflate. The solution state ^{19}F NMR spectrum of this complex showed a single signal at all temperatures between +20 and -50 °C suggesting rapid exchange of the coordinated and free triflate in solution. However, a solid state ^{19}F NMR spectrum showed two signals at -76.8 and -78.0 ppm consistent with the X-ray structure.

The formation of a five-coordinate complex from ligand **5** is probably due steric crowding caused by the 3,5-methyl groups on the bispyrazole coupled with non-planarity of the pyrazole rings which forces one of the bridging methylenes into the space required if the second triflate was bound to the zinc. The Zn–N and Zn–O bond lengths of the three complexes (Table 2) show the effect of having one of the two triflate ions dissociated from the metal with the complex of ligand **5** having much shorter bond lengths consistent with electron density being withdrawn from the ligands in order to stabilise the zinc. Dissociation of a triflate ion creates a vacant site and increases the Lewis acidity, which may explain the higher conversions achieved with the zinc complex of ligand **5**, despite the increased steric hindrance around the metal centre. The bite angle of the complexes of ligands **3** and **4** are very similar (78–79°), being restricted by the rigid geometry of the aromatic ring whilst the complex of ligand **5** has two different bite angles (88.5 and 91.1°) which are closer to 90°. This is achievable as the N–N distance is now larger and the methylene group between the pyrazoles also gives additional flexibility.

To further investigate the use of pyrazole ligands, methylenebis(3,5-di(*t*-butyl)pyrazole) **18** (Chart 2) was synthesised¹⁶ in an attempt to further increase the steric crowding around the zinc centre and possibly cause dissociation of both triflate ions, potentially enhancing the Lewis acidity and reactivity of the zinc. However, the resulting complex could not be crystallised and when one equivalent of ligand **18** was used with 5 mol% of zinc triflate to catalyse the addition of carbon dioxide to propylene glycol, only 28% conversion to propylene carbonate was achieved. This suggests that the *tert*-butyl groups are so sterically hindering, that either the ligand does not complex well to zinc, or the resulting zinc complex is too hindered to catalyse the reaction. The solution state NMR spectra did not allow the coordination

ARTICLE

number of the zinc ion to be determined as a single set of signals were seen in the ^1H , ^{13}C and ^{19}F NMR spectra, but a solid state ^{19}F NMR spectrum gave two signals at -78.6 and -79.7 ppm. These are analogous to those seen for the complex of ligand **5** and indicate that in the solid state the complex of ligand **18** is again five-coordinate with one coordinated and one free triflate ligand.

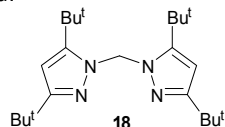
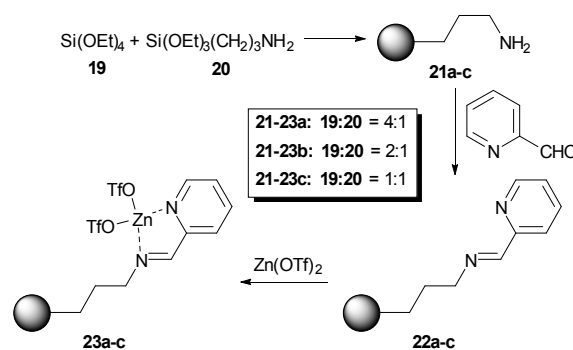
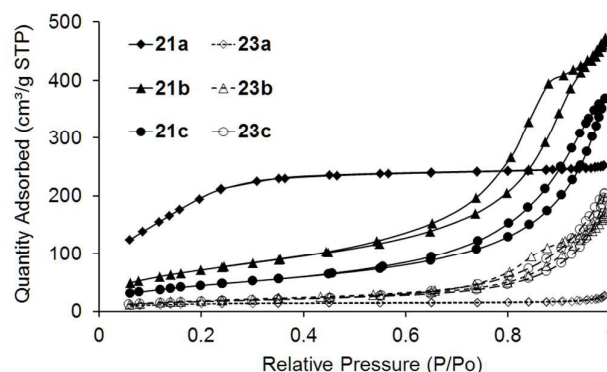
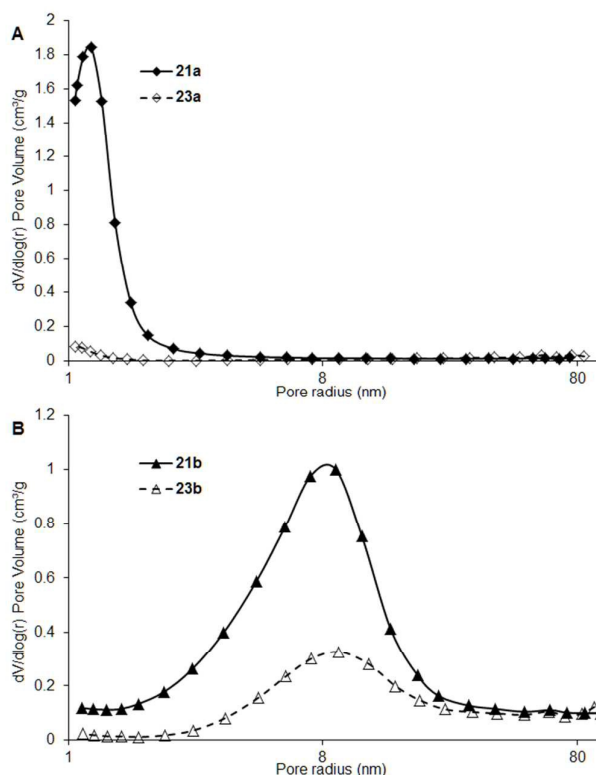
Chart 2: Structure of ligand **18**

Table 3: Zinc complexes as homogeneous catalysts for propylene carbonate synthesis.

Complex	Conversion (%)		2 yield (%)
	2	Acetates 15–17	
$[\text{Zn}(\mathbf{3})_2(\text{CF}_3\text{SO}_3)_2]$	31	29	29
$[\text{Zn}(\mathbf{4})_2(\text{CF}_3\text{SO}_3)_2]$	32	29	29
$[\text{Zn}(\mathbf{5})_2(\text{CF}_3\text{SO}_3)]^+(\text{CF}_3\text{SO}_3)^-$	40	38	37

The crystals of the zinc complexes of ligands **3–5** were used as catalysts for the synthesis of propylene carbonate from propylene glycol (Table 3) to investigate whether the isolated complexes had similar activity towards the carbonylation of diols with carbon dioxide to the *in situ* prepared complexes used in Table 1. The conversions for each ligand were similar irrespective of whether the zinc complex was prepared *in situ* or isolated and crystallised. This suggests that the catalytically active species has a single triflate ligand attached to the zinc since the *in situ* catalysts were prepared from a 1:1 ratio of zinc to ligand and the zinc complex of ligand **5** crystallised with a single ligand complexed to the zinc.

Having established that organozinc complexes of ligands **3–5** were active homogeneous catalysts for the synthesis of propylene carbonate, the heterogenisation of $\text{Zn}(\text{OTf})_2$ was investigated. Modification of commercial amorphous silica with 3-aminopropyltrimethoxysilane was initially investigated, but was found to give low loadings ($< 0.16 \text{ mmol g}^{-1}$) of the amine tether. Higher loadings of active species on the silica were necessary due to the quantity of catalyst (5 mol%) required to achieve good conversions to propylene carbonate. Therefore, three hexagonal mesoporous silicas **21a–c** were synthesised with aminopropyl tethers incorporated into the structure by a co-condensation sol gel process (Scheme 3).¹⁷ Three ratios (4:1, 2:1 and 1:1) of tetraethylorthosilicate **19** to 3-aminopropyltrimethoxysilane **20** were used in the preparation of silicas **21** to give materials with varying quantities of amine groups on the silica surface. 2-Pyridinecarboxaldehyde was reacted with silicas **21a–c** to give immobilised *N*-propyltriethoxysilane-1-(2-pyridyl) imines **22a–c**.¹⁸ This ligand was chosen due to the convenient synthesis of the silica-supported imine and the good results obtained with homogeneous imines of 2-pyridinecarboxaldehyde (**12** and **14**, see Table 1). Silica-supported imines **22a–c** were then stirred with a solution of zinc triflate in diethyl ether for 24 hours to give immobilised catalysts **23a–c**.¹⁸

Scheme 3: Synthesis of silica supported zinc complexes **21a–c**Figure 4: Isotherm linear plots of silicas **21a–c** and **23a–c**.

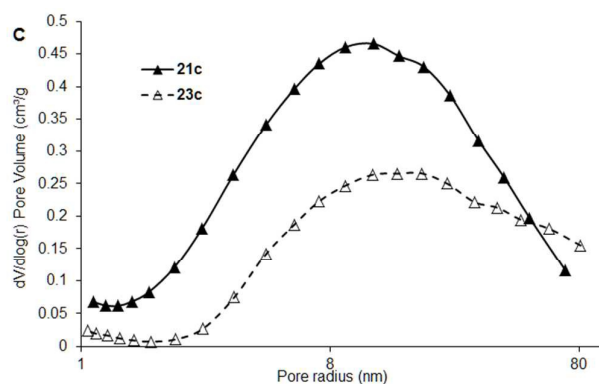


Figure 5: Pore size distributions of silicas **21-23a**, **21-23b** and **21-23c**

Porosimetry analysis of silicas **21** and **23** showed that a range of surface areas, pore size distributions and pore volumes were present (Table 4). Use of higher ratios of 3-aminopropyltrimethoxysilane **20** in the sol gel synthesis (**21-23b,c**) generally gave a large average pore diameter and low surface area mesoporous material. Each had a type four adsorption isotherm, with **21-23b** following a H2 type hysteresis loop (indicative of the material having a less well defined porous network) and **21-23c** tending towards H3 type (seen with aggregates of plate like particles).²⁰ The rapid rise of the isotherms around $p/p^0 = 1$ suggests the presence of macroporosity in the structures, more so for **21-23c** than for **21-23b**.

In contrast, silica **21a** was found to be highly microporous with minimal capillary condensation (mimicking a type one adsorption isotherm), showing lower pore volume and high surface area. After modifying each of silicas **21a-c** by formation of the 2-pyridyl imine ligand and subsequent complexation of zinc triflate, the surface area and pore volume decreased suggesting deposition within the porous network. Interestingly, the total quantity of zinc immobilised on each of the silicas was similar. Silica supported zinc complex **23a** showed a significant reduction in microporosity (Figure 5A) along with a large reduction in surface area (Figure 4). This implies that the microporous network had become blocked with zinc triflate, leading to increased zinc deposition on the external surface. Silica supported zinc complex **23b** showed a consistent and relatively broad but distinct pore size distribution in the mesoporous region with a slight reduction in pore volume, suggesting comparatively even dispersion of zinc triflate throughout the material. Silica supported zinc complex **23c** showed a slight increase in pore size distribution in the mesoporous and macroporous regions. Such an effect has been reported where deposited material aggregates around the entrance to the pore causing artificial widening to occur.²¹ Similarly, pore volume decreased suggesting deposition of zinc triflate within the pores.

Each of silicas **23a-c** were used as catalysts for the synthesis of propylene carbonate (Table 4). These heterogeneous catalysts were found to give lower yields of carbonate **2** than the homogeneous complexes. All gave a similar yield of compound **2** (18–26%) with **23a** giving the

lowest yield. This is most likely due to a high proportion of the zinc triflate being trapped within the microporous network and hence being inaccessible. Catalysts **23b** and **23c** gave essentially identical yields even though the porosimetry data suggested increased agglomeration of zinc triflate around the pore entrances of the latter.

Silica supported zinc complex **23b** was chosen to assess catalyst reusability as it achieved the highest conversion to

Table 4: Porosimetry and ICP-MS data of silicas **21-23** and their catalytic activities.

Silica	Surface area (m ² g ⁻¹)	Pore volume ^a (cm ³ g ⁻¹)	[Zn] (mmol g ⁻¹) ^b	2 yield (%) ^c
21a	783	0.39	-	-
21b	268	0.71	-	-
21c	167	0.56	-	-
23a	43	0.035	1.36	18
23b	66	0.25	1.46	26
			0.877 ^d	19 ^d
23c	63	0.30	1.49	25
			0.384 ^e	8 ^e

a) Single point adsorption total pore volume b) Determined by ICP-MS; c) Reaction conditions: 5 mol% equivalent zinc catalyst, propylene glycol 60 mmol, acetonitrile (10 mL), CO₂ (35 bar), 135 °C, 16 hours; d) Second use of catalyst isolated by filtration, washing with MeCN and drying at 100 °C for two hours; e) Third use of catalyst.

propylene carbonate **2**. The reisolated catalyst was washed with acetonitrile between uses and then dried in an oven at 100 °C before use. Yields of propylene carbonate **2** were found to reduce after each use due to leaching of the zinc from the silica caused by the polarity of the reaction mixture (propylene glycol and acetonitrile) along with the elevated reaction temperature used. This was supported by ICP-MS analysis of the supported zinc catalyst which showed that the zinc loading decreased by 0.6 mmol g⁻¹ after each use of the catalyst. In addition, a control experiment was carried out in which complex **23b** was suspended in acetonitrile and propylene glycol and heated to 135 °C under nitrogen in the absence of carbon dioxide. XRF analysis of complex **23b** before and after this treatment showed that the zinc content reduced from 23% to 19% consistent with leaching being due to the polar reaction mixture and not to the presence of carbon dioxide.

Conclusions

This study has shown three crystalline organozinc complexes to be active as catalysts for the synthesis of propylene carbonate from propylene glycol and carbon dioxide. The most active of these was [Zn(5)₂(CF₃SO₃)⁺](CF₃SO₃)⁻ which was shown by X-ray crystallography to possess a five coordinate zinc and a dissociated triflate anion. This configuration is thought to increase the catalytic activity of the zinc by enhancing its Lewis acidity, despite the increased steric crowding around the metal centre. Use of the even more sterically hindered ligand **18** resulted in reduced catalytic activity showing the need to balance steric and electronic effects in the ligand design. Use of ligands containing either an alcohol or ketone gave complexes with no catalytic activity, demonstrating how oxophilic the zinc is in this system.

ARTICLE

Journal Name

Similarly, the choice of the zinc counter ion is important for good catalytic activity with triflate being far superior to acetate.

Three aminopropyl functionalised silicas were prepared and modification of the amine groups to give pyridyl imine ligands followed by immobilisation of zinc triflate onto these silicas was successful, although deposition of the zinc varied between the materials. Porosimetry data suggested that the microporosity of silica **23a** caused the majority of zinc to aggregate on the external silica surface. Conversely, silica **23c** synthesised using the highest ratio of 3-aminopropyltrimethoxysilane to tetraethylorthosilicate was found to have increased quantities of zinc triflate aggregated around the pore entrances. Silica **23b** was found to have minimal macroporosity and a reproducible pore size distribution post modification suggesting relatively uniform dispersion of zinc throughout the material. All of the modified silicas were found to be catalytically active for the synthesis of propylene carbonate from propylene glycol and carbon dioxide. However, upon reuse silica **23b** was found to leach zinc, which may be attributed to the very polar reaction mixture.

Experimental

All reagents were commercially available (Alfa Aesar, Sigma-Aldrich, Fluka, TCI or Acros) and were used as received. Ligands **5**, **7**, **12–14** and **18** were prepared by a literature procedure.²² The zinc triflate used was anhydrous; see supplementary material for further information. Carbon dioxide was purchased from BOC. ¹H and ¹³C NMR spectra were recorded on a Jeol Oxford 400 at resonance frequencies of 400 MHz and 100 MHz respectively. ¹⁹F NMR spectra were recorded on a Bruker AVIHD500 spectrometer at 470 MHz. Solid state ¹⁹F spectra were recorded on a Bruker Avance III HD 400 at 377 MHz. Fluorine spectra are referenced relative to CFCl₃. X-ray crystallography was performed on a single-crystal Oxford Diffraction SuperNova with dual Mo & Cu sources at 110 K and a Bruker D8 powder diffractometer equipped with a Cu source at room temperature. Porosity data was obtained using a Micrometrics ASAP 2020 surface area and porosity analyser. Infrared spectroscopy of organic compounds was performed at a resolution of 1 cm⁻¹ using a Specac Quest ATR FTIR with a Bruker Vertex 70 Infrared Spectrometer. DRIFTS analysis of inorganic materials and heterogeneous catalysts was performed on a Bruker Equinox 55 using a resolution of 2 cm⁻¹ and a KBr dilution of 10:1. Melting points were obtained using a Gallenkamp melting point apparatus. Mass spectra were obtained using a Bruker micrOTOF time of flight mass spectrometer with ESI and APCI sources and an Agilent 1200 series LC system.

Synthesis of propylene carbonate using homogeneous complexes derived from zinc triflate.

Propylene glycol (4.56 g, 60 mmol), MeCN (10 mL), zinc triflate (1.06 g, 3 mmol), and ligand **3–14** (3 mmol) were added

to a predried stainless steel Parr reactor. The vessel was pressurised to 5 bar with CO₂ and heated to 135 °C. Once this temperature had been reached, the reactor was pressurised to 40 bar. After 16 hours, the reactor was cooled to room temperature and the pressure released. Acetonitrile was removed under reduced pressure and a sample of the residue was dissolved in d₆-DMSO for ¹H NMR analysis. The residue was purified by flash column chromatography using CH₂Cl₂ as eluent to give propylene carbonate **2** as a colourless liquid. δ_H(CDCl₃) 4.85–4.73 (m, 1H), 4.49 (ddt *J* 8.4, 7.6, 1.2 Hz, 1H), 3.95 (ddt *J* 8.5, 7.2, 1.3 Hz, 1H), 1.40 (dt *J* 6.3, 1.4 Hz, 3H). δ_C(CDCl₃) 155.2, 73.8, 70.8, 19.4. IR (ATR): 2991 and 1785 cm⁻¹. HRMS (ESI-TOF) *m/z*: [M+Na]⁺ Calcd. for C₄H₆O₃Na 125.0209; Found 125.0212.

Synthesis of [Zn(5)₂(CF₃SO₃)⁺ (CF₃SO₃)⁻].

Ligand **5** (0.22 g, 1.1 mmol) was stirred with anhydrous zinc triflate (0.18 g, 0.5 mmol) in dry MeCN (2 mL). After 16 hours, the complex was precipitated by addition of Et₂O. For X-ray diffraction analysis, the complex was crystallised from MeCN by vapour diffusion of Et₂O; the crystals were filtered and washed with Et₂O. δ_H(CD₃CN) 6.30 (s, 2H), 6.11 (s, 2H), 2.45 (s, 6H), 1.71 (s, 6H). δ_C(CD₃CN) 152.53, 144.4, 107.7, 56.9, 30.0, 11.6, 10.3. δ_F(CD₃COCD₃) -79.18 (s) at 298 K; -79.33 (s) at 223 K. δ_F(solid state) -76.8 and -78.0. Mp 235.4–236.9 °C. IR(ATR): 1559, 1466, 1389, 1306, 1278, 1254, 1228, 1205, 1152, 1030, 1019, 685, 636 and 574 cm⁻¹. HRMS (ESI-TOF) *m/z*: [M⁺] Calcd. for C₂₃H₃₂F₃N₈O₃SZn 621.1556; Found 621.1553.

Synthesis of complex from ligand **18** and Zn(OTf)₂.

Ligand **18** (0.050 g, 0.134 mmol) was stirred with anhydrous zinc triflate (0.024 g, 0.067 mmol) in dry Me₂CO (5 mL). After 16 hours, the solvent was evaporated in vacuo to leave a pale yellow solid. δ_H((CD₃CO)₂) 6.46 (s, 2H), 5.97 (s, 2H), 1.30 (s, 18H), 1.19 (s, 18H). δ_C((CD₃CO)₂) 158.9, 152.8, 101.2, 65.3, 31.7, 31.6, 29.9, 28.8. δ_F((CD₃CO)₂) -78.97 (s). δ_F(solid state) -78.6 and -79.7. Mp 130.1–131.9 °C. IR(ATR): 2964, 1637, 1543, 1462, 1363, 1313, 1282, 1228, 1181, 1029, 1016, 800, 774, 766 and 632 cm⁻¹. HRMS (ESI-TOF) *m/z*: [M⁺] Calcd. for C₅₁H₉₁N₈OZn [(**18**)₂ZnOMe]⁺ 895.6607; Found 895.6189.

Synthesis of aminopropyl functionalised silicas **21a–c**.

To a solution of n-dodecylamine (5.08 g, 27.5 mmol) dissolved in water–ethanol (53 ml water, 46 ml ethanol) were added, at room temperature, separately but simultaneously, tetraethylorthosilicate and 3-aminopropyltrimethoxysilane in quantities such that a total of 0.1 mole of silicon was added with the ratio required to give the desired degree of functionalisation. The initially clear solution became a thick white paste after 18 hours. The white solid was filtered and extracted with ethanol using a Soxhlet extractor (16 hours overnight). The remaining solid was collected and dried at 110 °C to give the aminopropyl functionalised silicas **21a–c** as white solids. For **21a**: DRIFTS 10:1 KBr dilution: 3737, 3363, 3293, 2939, 2868 and 1070 cm⁻¹. BET surface area: 783 m²/g, Single point adsorption total pore volume at P/Po = 0.98: 0.39 cm³/g,

BJH adsorption average pore radius: 1.1 nm. For **21b**: DRIFTS: 3755, 3364, 3299, 2936, 2864 and 1051 cm^{-1} . BET surface area: 268 m^2/g , Single point adsorption total pore volume at $P/P_0 = 0.99$: 0.71 cm^3/g , BJH adsorption average pore radius: 5.2 nm. For **21c**: DRIFTS: 3736, 3364, 3299, 2932, 2859 and 1049 cm^{-1} . BET surface area: 167 m^2/g , Single point adsorption total pore volume at $P/P_0 = 0.98$: 0.56 cm^3/g , BJH adsorption average pore radius: 6.5 nm.

Synthesis of silica supported ligands **22a–c**.

Aminopropyl functionalised silica **21a–c** (4 g) was added to a round bottom flask along with 2-pyridinecarboxaldehyde (12–22 mmol depending on the aminopropyl loading) and absolute ethanol (40 mL). The mixture was heated to reflux for 16 hours, then cooled to room temperature and filtered. The resulting solid was washed three times with hot ethanol and dried under reduced pressure at 50 $^\circ\text{C}$ until a free flowing powder formed. For **22a**: DRIFTS: 3759, 3365, 3293, 2978, 2939, 1653, 1596, 1571, 1474, 1448 and 1072 cm^{-1} . For **22b**: DRIFTS: 3753, 3360, 3293, 2936, 2889, 1651, 1588, 1559, 1469, 1439 and 1054 cm^{-1} . For **22c**: DRIFTS: 3744, 3278, 2935, 2887, 1650, 1590, 1589, 1470, 1437 and 1056 cm^{-1} .

Synthesis of silica supported zinc complexes **23a–c**.

Silica supported ligand **22a–c** and anhydrous zinc triflate (7.27 g, 20 mmol) were added to Et_2O (30 mL) and stirred at RT for 48 h. Then the solid was filtered and washed four times with Et_2O . The resulting solid was dried under vacuum to give **23a–c** as pale yellow solids. ICP-MS analysis showed zinc concentrations of 1.36, 1.46, 1.49 mmol g^{-1} for **23a, b** and **c** respectively. For **23a**: DRIFTS: 3748, 3254, 2982, 1654, 1605, 1572, 1483 and 1037 cm^{-1} . BET surface area: 43 m^2/g , Single point adsorption total pore volume at $P/P_0 = 0.98$: 0.035 cm^3/g , BJH adsorption average pore radius: 2.8 nm. For **23b**: DRIFTS: 3746, 3254, 2982, 1655, 1603, 1572, 1450 and 1036 cm^{-1} . BET surface area: 66 m^2/g , Single point adsorption total pore volume at $P/P_0 = 0.99$: 0.25 cm^3/g , BJH adsorption average pore radius: 8.1 nm. For **23c**: DRIFTS: 3746, 3254, 2982, 1655, 1603, 1573, 1449 and 1027 cm^{-1} . BET surface area: 63 m^2/g , Single point adsorption total pore volume at $P/P_0 = 0.98$: 0.30 cm^3/g , BJH adsorption average pore radius: 10.2 nm.

Catalyst leaching test.

Propylene glycol (4.6 g, 60 mmol), dry acetonitrile (10 mL) and of catalyst **23b** (5 mol% equivalent) were added to a dry stainless steel Parr reactor. The reactor was sealed, evacuated and refilled with N_2 three times and charged to 5 bar with N_2 . It was then heated to 135 $^\circ\text{C}$ achieving a final pressure of 10 bar. After 16 hours, the reactor was cooled to room temperature and the pressure released. The catalyst was filtered and washed four times with acetonitrile before being analysed by XRF. The % zinc content was found to reduce from 23.0% before the leaching test to 18.8% after the leaching test.

Acknowledgements

We gratefully acknowledge financial support from the European Union Seventh Framework Programme FP7–NMP–2012 under grant agreement number 309497 and Dr. Richard Heyn of SINTEF for helpful suggestions.

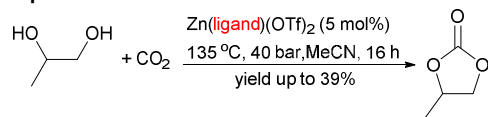
Notes and references

‡ Crystallographic data has been submitted to CCDC and compounds **3–5** given codes CCDC-1448143, CCDC-1448144 and CCDC-1448145 respectively.

- 1 B. Scrosati, J. Hassoun and Y.-K. Sun, *Energy Environ. Sci.*, 2011, **4**, 3287–3295; V. Aravindan, J. Gnanaraj, S. Madhavi and H.-K. Liu, *Chem. Eur. J.*, 2011, **17**, 14326–14346.
- 2 B. Nohra, L. Candy, J. F. Blanco, C. Guerin, Y. Raoul and Z. Mouloungui, *Macromolecules*, 2013, **46**, 3771–3792; M. Yadollahi, H. Bouhendi, M. J. Zohuriaan-Mehr, H. Farhadnejad and K. Kabiri, *Polym. Sci. B*, 2013, **55**, 327–335; W. Guerin, A. K. Diallo, E. Kirilov, M. Helou, M. Slawinski, J.-M. Brusson, J.-F. Carpentier and S. M. Guillaume, *Macromolecules*, 2014, **47**, 4230–4235.
- 3 J. O. Jun, J. Lee, K. H. Kang and I. K. Song, *J. Nanosci. Nanotechnol.*, 2015, **15**, 10, 8330–8335; P. Wang, S. Liu, F. Zhoua, B. Yanga, A. S. Alshammari, L. Lu and Y. Deng, *Fuel Process. Technol.*, 2014, **126**, 359–365.
- 4 C. Lian, F. Ren, Y. Liu, G. Zhao, Y. Ji, H. Rong, W. Jia, L. Ma, H. Lu, D. Wanga and Y. Li, *Chem. Commun.*, 2015, **51**, 1252–1254
- 5 C. Beattie, M. North and P. Villuendas, *Molecules*, 2011, **16**, 3420–3432; H. L. Parker, J. Sherwood, A. J. Hunt and J. H. Clark, *ACS Sustainable Chem. Eng.*, 2014, **2**, 1739–1742; J. A. Castro-Osma, J. W. Comerford, S. Heath, O. Jones, M. Morcillo and M. North, *RSC Adv.*, 2015, **5**, 3678–3685.
- 6 J. W. Comerford, I. D. V. Ingram, M. North and X. Wu, *Green Chem.*, 2015, **17**, 1966–1987; M. Cokoja, M. E. Wilhelm, M. H. Anthofer, W. A. Herrmann and F. E. Kuhn, *ChemSusChem*, 2015, **8**, 2436–2454; Q. He, J. W. O'Brien, K. A. Kitzelman, L. E. Tompkins, G. C. T. Curtis and F. M. Kerton, *Cat. Sci. Tech.*, 2014, **4**, 1513–1528; A. Decortes, A. M. Castilla and A. W. Kleij, *Angew. Chem. Int. Ed.*, 2010, **49**, 9822–9837.
- 7 J. Martinez, J. A. Castro-Osma, C. Alonso-Moreno, A. Otero, A. Lara-Sanchez, M. North and A. Rodriguez-Dieguez, *Chem. Eur. J.*, 2015, **21**, 9850–9862; J. A. Castro-Osma, M. North and X. Wu, *Chem. Eur. J.*, 2014, **20**, 15005–15008; I. S. Metcalfe, M. North and P. Villuendas, *J. CO₂ Util.*, 2013, **2**, 24–28; M. North, *ARKIVOC*, 2012, (i), 610–628; M. North and C. Young, *ChemSusChem*, 2011, **4**, 1685–1693; J. A. Castro-Osma, M. North and X. Wu, *Chem. Eur. J.*, 2016, **22**, 2100–2107.
- 8 M. Tamura, M. Honda, Y. Nakagawa and K. Tomishige, *J. Chem. Technol. Biotechnol.*, 2014, **89**, 19–33; J. A. Castro-Osma and M. North, *Curr. Green Chem.*, 2014, **1**, 257–272.
- 9 K. Müller, L. Mokrushina and W. Arlt, *Chem. Ing. Tech.*, 2014, **86**, 497–503.
- 10 M. Honda, M. Tamura, Y. Nakagawa and K. Tomishige, *Catal. Sci. Technol.* 2014, **4**, 2830–2845.
- 11 J. A. Castro-Osma, J. W. Comerford, R. H. Heyn, M. North and E. Tangstad, *Faraday Discussions*, 2015, **183**, 19–30.
- 12 X. Zhao, N. Sun, S. Wang, F. Li and Y. Wang, *Ind. Eng. Chem. Res.* 2008, **47**, 1365–1369.

- 13 M. Honda, M. Tamura, K. Nakao, K. Suzuki, Y. Nakagawa and K. Tomishige, *ACS Catal.* 2014, **4**, 1893–1896.
- 14 C. Obuaha, Y. Locheea, O. Zinyembaa, J. H. L. Jordaanb, D. P. Ottob, and J. Darkwaa, *J. Mol. Catal. A: Chem.*, 2015, **406**, 185–193; X. X. Zheng, C. Zhang and Z. X. Wang, *J. Organomet. Chem.*, 2015, **783**, 105–115.
- 15 J. Borner, U. Florke, A. Doring, D. Kuckling, M. D. Jones and S. Herres-Pawlis, *Sustainability*, 2009, **1**, 1226–1239.
- 16 Z. Zhang, D. Cui and A. A. Trifonov, *Eur. J. Inorg. Chem.*, 2010, **18**, 2861–2866.
- 17 D. J. Macquarrie, *Green Chem.*, 1999, **1**, 195–198.
- 18 E. B. Mubofu, J. H. Clark and D. J. Macquarrie, *Green Chem.*, 2001, **3**, 23–25.
- 19 For the synthesis of a similar complex see: M. D. Serio, G. Carotenuto, M. E. Cucciolo, M. Lega, F. Ruffo, R. Tesser and M. Trifuoggi, *J. Mol. Catal. A: Chem.*, 2012, **353–354**, 106–110.
- 20 K. S. W. Sing, D. H. Everett; R. A. W. Haul, L. Moscou, R. A. Pierotti, J. Rouquerol and T. Siemieniewska, *Pure Appl. Chem.*, 1985, **57**, 603–619; J. C. P. Broekhoff, *Stud. Surf. Sci. Catal.*, 1979, **3**, 663–684; J. E. Shields, S. Lowell, M. A. Thomas and M. Thommes, *Characterization of Porous Solids and Powders: Surface Area, Pore Size and Density*, Kluwer Academic Publisher, Boston, MA, USA, 2004, 43–45.
- 21 A. R. Silva, V. Budarin and J. H. Clark, *ChemCatChem*, 2013, **5**, 895–898.
- 22 Literature preparations for complexes as follows: **5** and **18** see reference 16; **7** G. Volpi, C. Garino and C. Nervi, *Dalton Trans.*, 2012, **41**, 7098–7108; **12–14** see reference 19.

Graphical abstract



13 homogeneous ligands and 3 silica supported ligands investigated



Homogeneous and silica-supported zinc triflate complexes catalyse the synthesis of propylene carbonate from propane-1,2-diol and carbon dioxide.